SUPPLEMENTARY MATERIAL

MS Title “A Definitive Assessment of the CO Oxidation Pattern of a Nanocomposite MnCeO$_x$ Catalyst”

Authors: F. Arena, R. Di Chio, C. Espro, A. Palella, L. Spadaro

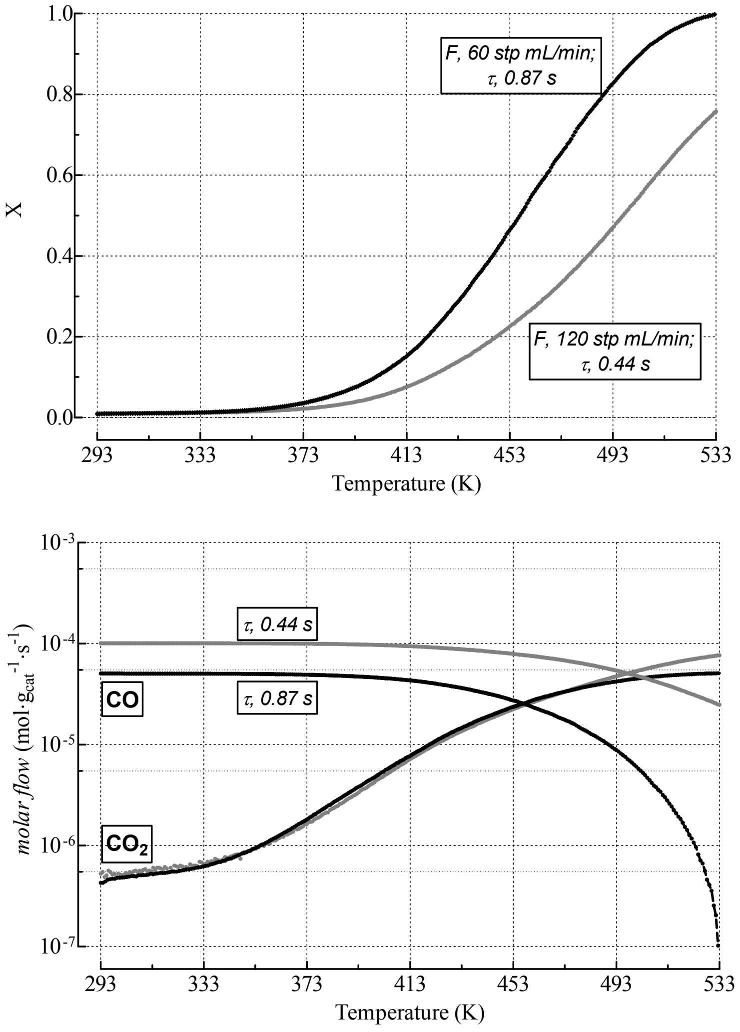

Fig. S1. CO conversion (top) and CO$_x$ molar flow (bottom) of the M5C1 catalyst in the range of 293-533K *(w_{cat}, 0.02 g; F, 60-120 stp mL/min; p^0_{CO}, 0.025; λ_0, 1)*. Effect of the feed flow rate.

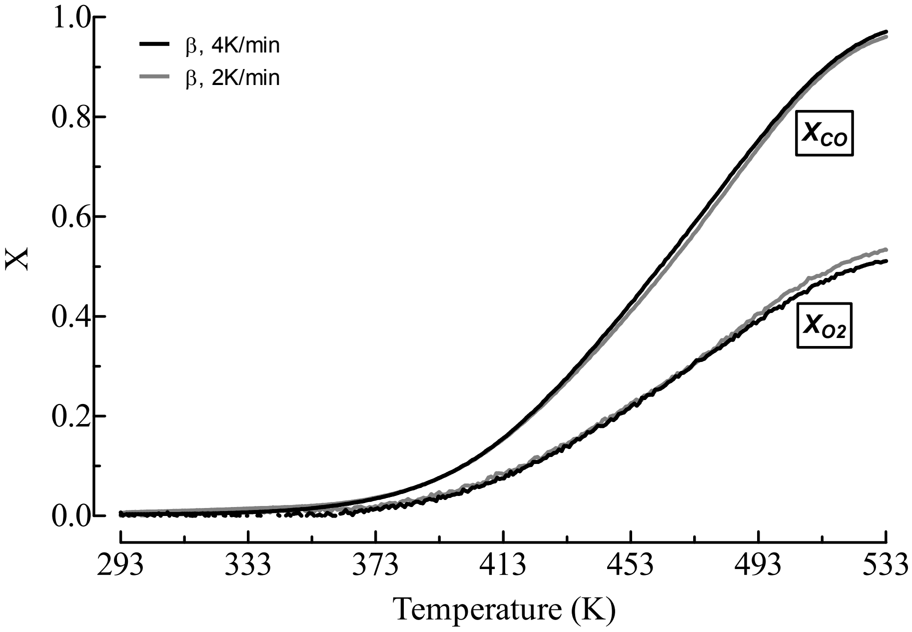

Fig. S2. CO conversion data of the M5C1 catalyst in the range of 293-533K *(w_{cat}, 0.02 g; F, 60 stp mL/min; p^0_{CO}, 0.025; λ_0, 1)*. Effect of the heating rate (β).

Appendix A

Experimental Parameters and Calculations for Mass-Transfer Resistances Evaluation

Mass transfer resistances on the reaction kinetics of the M5C1 catalyst were probed considering a CO a conversion of 80% at 493K (Fig. 1A), applying the following criteria:

Resistance	**Criterion**	**Relationship**	**Source**
External diffusion	*Mears*	$C_M = \frac{-r_{CO}\cdot\rho_b\cdot R\cdot n}{k_c\cdot C_{CO,b}} < 0.15$	a
Internal diffusion	*Weisz-Prater*	$C_{WP} = \frac{-r_{CO,obs}\cdot\rho_c\cdot R^2}{D_e\cdot C_{CO,s}} < 1$	a
Axial Dispersion	*Mears*	$\frac{L_b}{d_p} \geq \frac{20\cdot n}{Pe}\cdot ln\left(\frac{C_{in}}{C_{out}}\right)$	a

a) D.E. Mears, Ind. Eng. Chem., Process Des. Dev., 1971, 10, 541.

where
$-r_{CO}$ = reaction rate (**$4.2\cdot10^{-5}$ kmol·$kg_{cat}^{-1}\cdot s^{-1}$**);
S = total surface area (**159 m^2/g**)
n = reaction order (**1st**);
R = catalyst particle radius, m (**$2.5\cdot10^{-5}$ m**);
ρ_b = bulk density of the catalyst bed, kg/m^3 (**900 kg/m^3**);
ε_b = porosity or void fraction of the packed bed (**0.2**);
ε_p = porosity or void fraction of the catalyst particle (**0.6**);
ρ_p = catalyst particle density, kg/m^3 (**1,100 kg/m^3**);
ρ_c = solid catalyst density, kg/m^3 (**3,300 kg/m^3**);
$C_{CO,b}$ = bulk gas concentration of CO, kmol/m^3. Note: if external diffusion is negligible, $C_{CO,s}$=$C_{CO,b}$;
k_c = mass transfer coefficient, m/s;
τ, tortuosity factor (**3**);
σ_c, constriction factor (**0.5**);
D_e = effective mass transfer coefficient inside the catalyst particle, m^2/s, given by the formula:

$$\frac{1}{D_e} = \frac{1}{D_{CO/He,eff}} + \frac{1}{D_{Knudsen}}$$

$$where\ ,\ D_{CO/He,eff} = \frac{D_{CO/He}\cdot\varepsilon_p\cdot\sigma_c}{\tau} = 4\cdot10^{-6}\ m^2/s;\quad D_{Knudsen} = 19{,}400\cdot\frac{\varepsilon_p^2}{\tau\cdot S\cdot\rho_p}\cdot\sqrt{\frac{T}{PM_{CO}}} = 6\cdot10^{-7}\ m^2/s$$

The following experimental parameters values were considered for calculations

Parameter	**Experimental Value**	**Source**
F (stp mL/min)	60 *stp* mL/min	exp. par.
Composition	He/CO/O_2=95/2.5/2.5	exp. par.
A.M.W. of reaction mixture	5.3 kg/kmol	exp. par.
d_{int} *(m)*	$4\cdot10^{-3}$ m	exp. par.
v_s *(m/s)*	$8\cdot10^{-2}$ m/s @ 298K	exp. par.
L_b	$2\cdot10^{-2}$ m	exp. par.
$D_{CO/He}$ *(m^2/s)*	$1.6\cdot10^{-4}$ m^2/s @ 493K	calculated
D_e *(m^2/s)*	$5\cdot10^{-7}$ m^2/s @ 493K	calculated
$\mu_{(He)}$ *(N·s/m^2)*	$2.6\cdot10^{-5}$ N·s/m^2 @ 493K	b
ρ *(kg/m^3)*	0.22 kg/m^3 @ 298K; 0.13 kg/m^3 @ 493K	exp. par.
$C_{CO,b}$	$1.0\cdot10^{-3}$ kmol/m^3 @ 298K; $0.6\cdot10^{-3}$ kmol/m^3 @ 493K	exp. par.
d_p *(m)*	$5\cdot10^{-5}$ m	exp. par.

b) J.M. Coulson, J.F. Richardson, Chemical Engineering, vol. 1 - 4th Ed., Pergamon Press, 1990.

Number	**Relationship**	**Source**	**Calculated value**
Reynolds	$Re = \frac{\rho \cdot v_s \cdot d_p}{\left(1 - \varepsilon_b\right) \cdot \mu}$	c	*Re*, 0.043
Schmidt	$Sc = \frac{\mu}{\rho \cdot D_{CO/He}}$	c	*Sc*, 1.30
Sherwood	$Sh = \frac{0.499 \cdot Re^{0.618} \cdot Sc^{0.33}}{\varepsilon_b} = \frac{k_c \cdot d_p}{D_{CO/He}}$	c	*Sh*, 0.4; $k_c = 1.20\ m/s$
Peclet	$\frac{1}{Pe} = \frac{0.3}{Re \cdot Sc} + \frac{0.5}{1 + \frac{3.8}{Re \cdot Sc}}$	c	*Pe*, 0.20

c) Perry J.H. Chemical Engineers Handbook – 3rd/4th/5th edition McGraw-Hill Book Company, Inc.

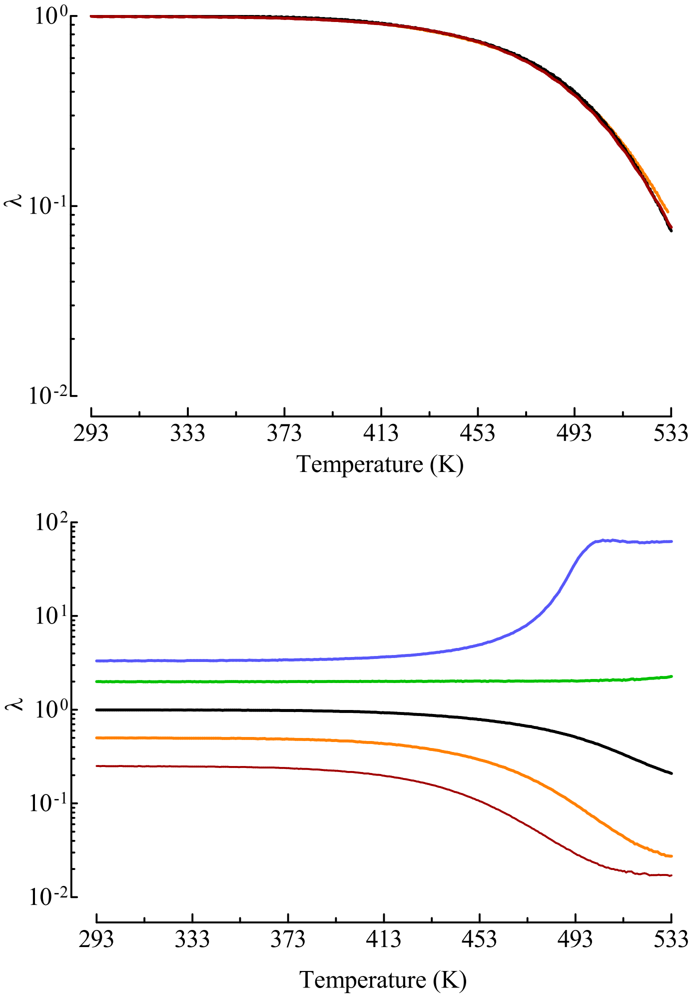

Fig. S3. λ factor for TPCR measurements (Fig. 1) at different reagent pressure (top) and λ_0 (bottom).

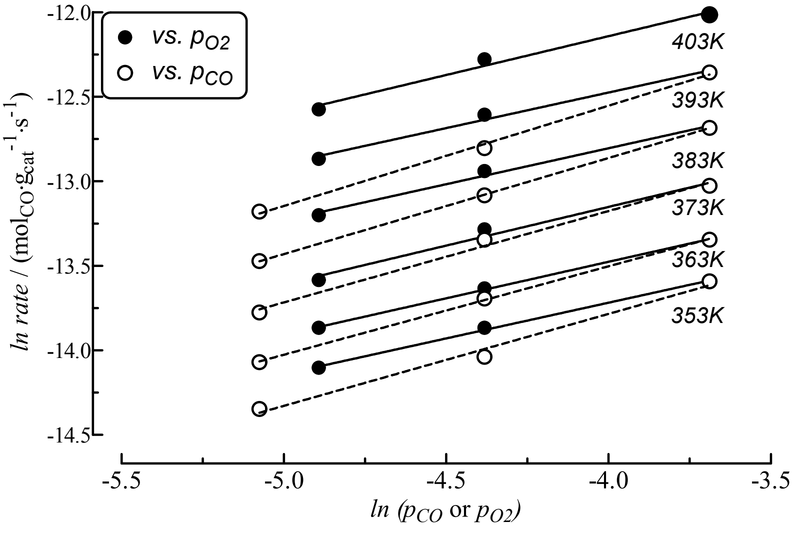

Fig. S4. Log-plot of kinetic data (X<10%) in the range of 353-403K (data from Fig. 1B).

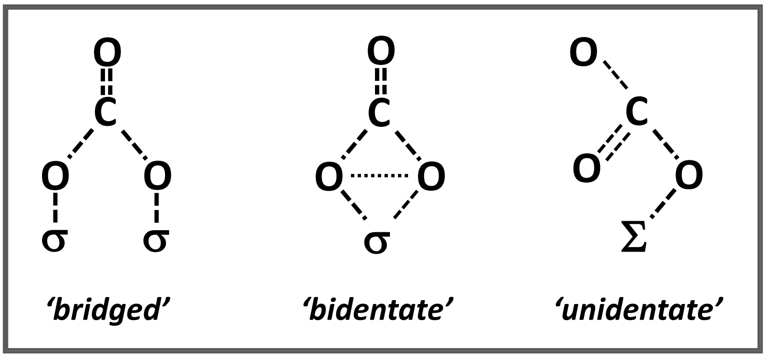

Fig. S5. Scheme of carbonate intermediates forming at the surface of TMO systems [*adapted from ref. 29*].

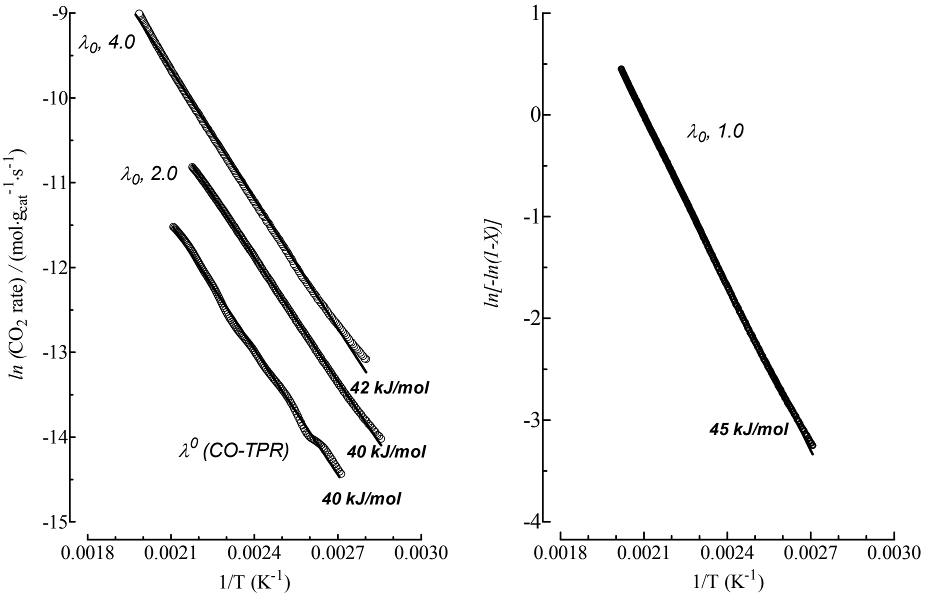

Fig. S6. Arrhenius plots of CO_2 rate data at different λ_0 (left), and elaboration of conversion data (λ_0, 1) in the range of 293-533K by the integral 1st-order model [ref. 13] (right).

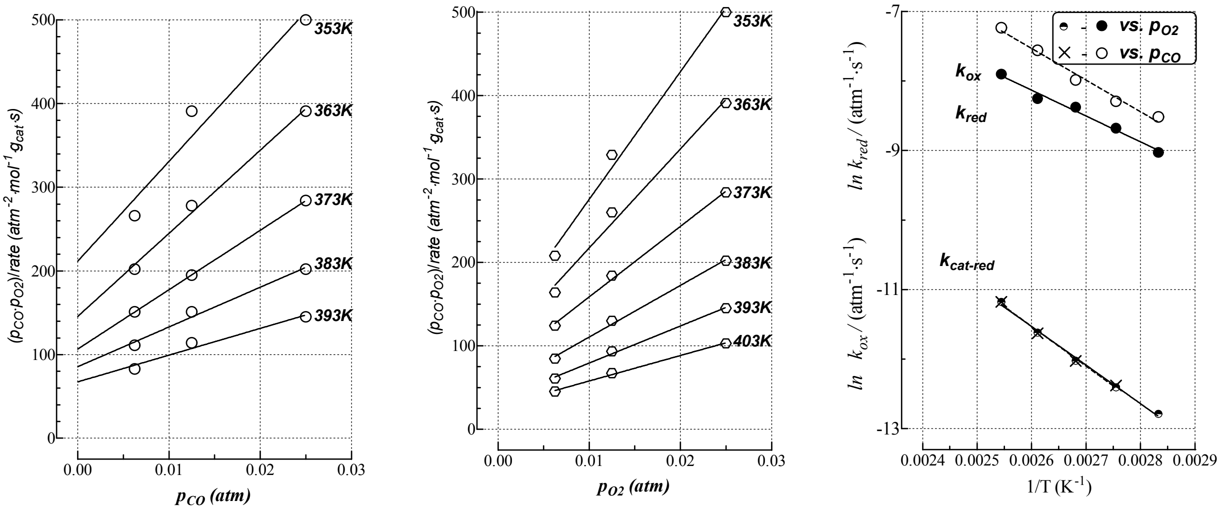

Fig. S7. Elaboration of kinetic data in the range of 353-403K by eq. 7 as a function of p_{CO} (left) and p_{O2} (center) and Arrhenius plot of the kinetic constants k_2, k_3 and k_{CO2} (right).

Appendix B

- <u>Reaction Mechanism and Kinetic Modelling</u>

	Reaction Step	Approximation	Thermodynamic and kinetic relationship	Constant
a	$CO + \sigma O$ 👎 $CO \cdot O\sigma$	*q.e. (equilibrium)*	$K_1 = \frac{[\sigma OCO]}{p_{CO} \cdot [\sigma O]}$	K_1, atm^{-1}
b	$CO \cdot O\sigma$ ✂ $CO_2 + \sigma$	*r.d.s. (slow)*	$r_2 = k_2 \cdot [\sigma OCO]$	k_2, $mol \cdot g_{cat}^{-1} \cdot s^{-1}$
c	$\sigma + O_2$ ✂ σO_2	*i.s. (fast)*	$r_3 = k_3 \cdot p_{O_2} \cdot [\sigma]$	k_3, $mol \cdot g_{cat}^{-1} \cdot s^{-1} \cdot atm^{-1}$
d	$CO + \sigma O_2$ ✂ $CO_2 \cdot \sigma O$	*i.s. (fast)*	$r_4 = k_4 \cdot p_{CO} \cdot [\sigma O_2]$	k_4, $mol \cdot g_{cat}^{-1} \cdot s^{-1} \cdot atm^{-1}$
e	$CO_2 \cdot \sigma O$ 👎 $\sigma O + CO_2$	*q.e. (equilibrium)*	$K_5 = \frac{[\sigma OCO_2]}{[\sigma O] \cdot p_{CO_2}}$	K_5, atm^{-1}

- <u>Mass Balance on Surface Sites and Intermediates</u>

$$1 = [\sigma O] + [\sigma O \cdot CO] + [\sigma] + [\sigma O_2] + [\sigma O \cdot CO_2]$$

$$[\sigma O] = \frac{k_3 \cdot k_4 \cdot p_{O2}}{\left[k_3 \cdot k_4 \cdot p_{O2} + K_1 \cdot k_3 \cdot k_4 \cdot p_{O2} \cdot p_{CO} + K_1 \cdot k_2 \cdot k_4 \cdot p_{CO} + K_1 \cdot k_2 \cdot k_3 \cdot p_{O2} + K_5 \cdot p_{CO_2} \cdot k_3 \cdot k_4 \cdot p_{O2}\right]}$$

$$[\sigma OCO] = K_1 \cdot p_{CO} \cdot [\sigma O]$$

$$[\sigma] = \frac{K_1 \cdot k_2 \cdot p_{CO}}{k_3 \cdot k_4 \cdot p_{O2}} \cdot [\sigma O]$$

$$[\sigma O_2] = \frac{K_1 \cdot k_2}{k_4} \cdot [\sigma O]$$

$$[\sigma OCO_2] = K_5 \cdot p_{CO2} \cdot [\sigma O]$$

- <u>Rate Equation</u>

$$rate = \frac{K_1 \cdot k_2 \cdot k_3 \cdot k_4 \cdot p_{CO} \cdot p_{O_2}}{k_3 \cdot k_4 \cdot p_{O_2} + K_1 \cdot k_3 \cdot k_4 \cdot p_{CO} \cdot p_{O_2} + K_1 \cdot k_2 \cdot k_4 \cdot p_{CO} + K_1 \cdot k_2 \cdot k_3 \cdot p_{O_2}}$$

- <u>Linear Function of the Rate Equation</u>

$$\frac{p_{CO} \cdot p_{O_2}}{rate} = \frac{p_{O_2}}{(K_1 \cdot k_2)} + \frac{p_{O_2}}{k_4} + \frac{p_{CO} \cdot p_{O_2}}{k_2} + \frac{p_{CO}}{k_3}$$

- Relationships for Slope and Intercept of the Linear Function of the Rate Equation

$\frac{p_{CO} \cdot p_{O_2}}{rate} = f(p_{CO})$	$slope_{CO} = \left(\frac{1}{k_3} + \frac{1}{k_2} \cdot p_{O_2}\right)$ $intercept_{CO} = p_{O_2} \cdot \frac{1}{k_{CO_2}}$	$p_{O_2} = 0.025\ atm\ (cost.)$ $\frac{1}{k_{CO_2}} = \left(\frac{1}{(K_1 \cdot k_2)} + \frac{1}{k_4}\right)$
$\frac{p_{CO} \cdot p_{O_2}}{rate} = f\left(p_{O_2}\right)$	$slope_{O_2} = \left(\frac{1}{k_{CO_2}} + \frac{1}{k_2} \cdot p_{CO}\right)$ $intercept_{O_2} = p_{CO} \cdot \frac{1}{k_3}$	$p_{CO} = 0.025\ atm\ (cost.)$ $\frac{1}{k_{CO_2}} = \left(\frac{1}{(K_1 \cdot k_2)} + \frac{1}{k_4}\right)$

- Relationships for Calculation of the Kinetic Constants

$$\frac{1}{k_3} = \frac{intercept_{O_2}}{0.025}$$

$$\frac{1}{k_2} = \frac{slope_{CO} - \frac{1}{k_3}}{0.025}$$

$$\frac{1}{k_{CO_2}} = \frac{intercept_{CO}}{0.025}$$

$$\frac{1}{k_2} = \frac{slope_{O_2} - \frac{1}{k_{CO_2}}}{0.025}$$

$$\frac{1}{k_{CO_2}} = slope_{O_2} - \frac{1}{k_2} \cdot 0.025$$

Tab. S1. Slope and intercept values of the straight-line relationships obtained from kinetic data elaborated by the eq. 7, and kinetic constant values of the various reaction steps in the range of 353-403K.

T (K)	*slope*$_{CO}$	*intercept*$_{CO}$	*slope*$_{O2}$	*intercept*$_{O2}$	k_2 (mol·g$_{cat}^{-1}$·s^{-1})	k_3 (mol·g$_{cat}^{-1}$·s^{-1}·atm$_{O2}^{-1}$)	k_{CO2} (mol·g$_{cat}^{-1}$·s^{-1}·atm$_{CO}^{-1}$)
353	12,210±1426	200±24	14,170±471	147±8	$4.0\cdot10^{-6}$	$1.7\cdot10^{-4}$	$1.3\cdot10^{-4}$
363	9,931±772	146±13	10,970±471	118±1	$4.8\cdot10^{-6}$	$2.1\cdot10^{-4}$	$1.7\cdot10^{-4}$
373	7,097±20	107±1	8,757±396	89±4	$7.1\cdot10^{-6}$	$2.8\cdot10^{-4}$	$2.1\cdot10^{-4}$
383	4,743±574	86±10	6,194±376	58±1	$1.0\cdot10^{-5}$	$4.3\cdot10^{-4}$	$2.8\cdot10^{-4}$
393	3,198±622	67±10	4,445±267	42±1	$1.6\cdot10^{-5}$	$6.0\cdot10^{-4}$	$3.6\cdot10^{-4}$
403	n.d.	n.d.	3,051±162	33±1	n.d.	$7.6\cdot10^{-4}$	n.d

Tab. S2. Predicted values of the kinetic and thermodynamic constants of the various reaction steps in the range of 293-533K (see Fig. S7 and App. B of SI).

T (K)	k_2 ($mol \cdot g_{cat}^{-1} \cdot s^{-1}$)	k_3 ($mol \cdot g_{cat}^{-1} \cdot s^{-1} \cdot atm_{O2}^{-1}$)	k_{CO2} ($mol \cdot g_{cat}^{-1} \cdot s^{-1} \cdot atm_{CO}^{-1}$)
293	$1.4 \cdot 10^{-7}$	$9.4 \cdot 10^{-6}$	$8.5 \cdot 10^{-6}$
313	$4.7 \cdot 10^{-7}$	$2.7 \cdot 10^{-5}$	$2.3 \cdot 10^{-5}$
333	$1.3 \cdot 10^{-6}$	$6.8 \cdot 10^{-5}$	$5.3 \cdot 10^{-5}$
353	$3.6 \cdot 10^{-6}$	$1.6 \cdot 10^{-4}$	$1.2 \cdot 10^{-4}$
373	$7.1 \cdot 10^{-6}$	$3.0 \cdot 10^{-4}$	$2.1 \cdot 10^{-4}$
393	$1.6 \cdot 10^{-5}$	$5.9 \cdot 10^{-4}$	$4.0 \cdot 10^{-4}$
413	$3.1 \cdot 10^{-5}$	$1.1 \cdot 10^{-3}$	$6.9 \cdot 10^{-4}$
433	$5.9 \cdot 10^{-5}$	$1.9 \cdot 10^{-3}$	$1.2 \cdot 10^{-3}$
453	$1.0 \cdot 10^{-4}$	$3.1 \cdot 10^{-3}$	$1.9 \cdot 10^{-3}$
473	$1.7 \cdot 10^{-4}$	$4.9 \cdot 10^{-3}$	$2.8 \cdot 10^{-3}$
493	$2.8 \cdot 10^{-4}$	$7.4 \cdot 10^{-3}$	$4.2 \cdot 10^{-3}$
513	$4.5 \cdot 10^{-4}$	$1.1 \cdot 10^{-2}$	$6.2 \cdot 10^{-3}$
533	$6.6 \cdot 10^{-4}$	$1.6 \cdot 10^{-2}$	$8.5 \cdot 10^{-3}$

Appendix C

- Rate Equation

$$rate = \frac{K_1 \cdot k_2 \cdot k_3 \cdot k_4 \cdot p_{CO} \cdot p_{O_2}}{\left(k_3 \cdot k_4 \cdot p_{O_2} + K_1 \cdot k_3 \cdot k_4 \cdot p_{CO} \cdot p_{O_2} + K_1 \cdot k_2 \cdot k_4 \cdot p_{CO} + K_1 \cdot k_2 \cdot k_3 \cdot p_{O_2} + K_5 \cdot p_{CO2} \cdot k_3 \cdot k_4 \cdot p_{O_2}\right)}$$

- Apparent Activation Energy

$$E_{app} = RT^2 \cdot \frac{\partial ln(rate)}{\partial T} = RT^2 \cdot \frac{\partial}{\partial T}\left[ln(p_{CO} \cdot p_{O2}) + ln(K_1) + ln(k_2) + ln(k_3) + ln(k_4) - ln(.....)\right] =$$

$$= RT^2 \cdot \left[0 + \frac{\partial\left(-\frac{\Delta H_1}{RT}\right)}{\partial T} + \frac{\partial\left(-\frac{E_2}{RT}\right)}{\partial T} + \frac{\partial\left(-\frac{E_3}{RT}\right)}{\partial T}\frac{\partial\left(-\frac{E_4}{RT}\right)}{\partial T} - \frac{\left[\frac{\partial}{\partial T}(.....)\right]}{(.....)}\right] =$$

$$= \Delta H_1 + E_2 + E_3 + E_4 - [\sigma O] \cdot (E_3 + E_4) - [\sigma O_2] \cdot (\Delta H_1 + E_2 + E_3) - [\sigma OCO_2] \cdot ($$
$$\cdot (\Delta H_1 + E_3 + E_4)$$

According to model assumptions, the concentration of the following intermediates at steady-state can be considered negligible

$$[\sigma O \cdot\cdot CO] \approx [\sigma] \approx [\sigma O_2] \approx 0$$

And therefore the above relationship leads to the conclusion that the apparent activation barrier has the following meaning

$$E_{app} = \Delta H_1 + E_2 - [\sigma OCO_2] \cdot (\Delta H_5)$$

Showing that in absence of CO_2 the apparent energetic barrier reflects the resistance to reduction of surface active Mn^{IV} sites.

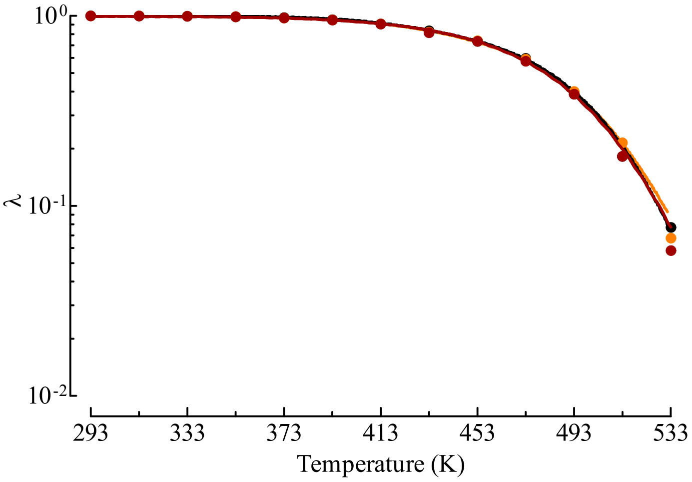
10^0
10^{-1}
10^{-2}
λ
293
333
373
413
453
493
533
Temperature (K)

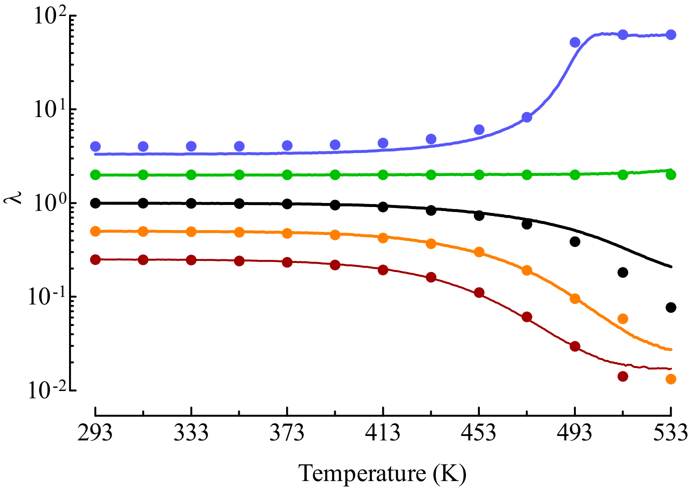
10^2
10^1
10^0
10^{-1}
10^{-2}
λ
293
333
373
413
453
493
533
Temperature (K)

Fig. S8. Predicted (symbols) and experimental λ data (lines) at different reagent concentration (top) and λ_0 values (bottom) in the range of 293-533K.